Transactions, SMiRT-22
San Francisco, California, USA - August 18-23, 2013
Division V

HIGH-TEMPERATURE CANDU FUEL PIN DEFORMATION: EXPERIMENT AND MODEL

Catherine M. Thiriet[1], Raymond S. Dickson[2], Anthony F. Williams[2], and Karen D. Colins[2]

[1] Research Scientist, Reactor Safety Division, Atomic Energy of Canada Limited, Chalk River, ON (thirietc@aecl.ca)
[2] Research Scientist, Reactor Safety Division, Atomic Energy of Canada Limited, Chalk River, ON

ABSTRACT

Due to the horizontal orientation of CANDU® fuel channels, the fuel pins, which are assembled in bundles, may deform (sag) by gravity during high-temperature abnormal reactor events. Because excessive fuel pin and bundle deformation may affect the progression and consequences of potential accidents, a significant experimental and modeling program, mainly funded by CANDU® Owners Group (COG), has been started at Atomic Energy of Canada Limited (AECL). The unique experimental set-up and instrumentation used for high-temperature single fuel pin deformation tests are presented in this paper. The deflection was measured by a laser light-stripe sensor travelling along the pin length. The fuel pin was supported near its ends and heated at about 1°C/s. Its deflection became readily detectable when the temperature reached 760 ± 10°C. The sag rate was between 0.019 and 0.010±0.002 mm/s during 120 s hold periods at 800°C. During continued heating at 1°C/s, the sag rate increased significantly to about 0.20±0.01 mm/s at temperatures above 870°C. The fuel pin sagged by >28 mm to contact the furnace tube at 970°C before reaching the 1000°C plateau. Experimental results of the fuel pin sag test have been compared with those of a computer simulation of the test using ANSYS models.

INTRODUCTION

Due to the horizontal orientation of CANDU® fuel channels, the fuel pins, which are assembled in bundles, may deform (sag) by gravity during high-temperature abnormal reactor events (Kohn et al. (1985)). Thermal and mechanical loads may be transferred from fuel pins to the pressure tube (Walters and Williams (2003)). Dry and hot patches can then develop on the fuel pin surface and pressure tube, potentially leading to core damage. Because the fuel pins are assembled in a bundle, their deformation will restrict the coolant flowing through the bundle subchannels. Therefore, by reducing the bundle coolability, its temperature will increase and lead to further deformation.

A significant experimental and modeling program, mainly funded by CANDU® Owners Group (COG), has been started at Atomic Energy of Canada Limited (AECL) to determine sag rates for well-characterized individual fuel pins and to model those tests, in order to provide validation data and models for fuel pin sag at high temperatures. As deformation due to end-plate settling and fuel pin/fuel pin contact can be significant, the future experiments and model development will include an entire 37-pin bundle. The single fuel pin sag test presented in this paper is considered as a reference test because no alteration of its mechanical integrity has been made before the test and the fuel pin was simply supported with neither axial nor rotational constraints (the simplest support configuration).

The fuel pin sag experiment will be presented, including a description of the material, equipment and instrumentation used as well as the temperature transients applied to the fuel pin. Then, the analysis of the spatiotemporal multi-dimensional data collected during heating using a non-intrusive dimensioning system will be described and results reported. Finally a model using the ANSYS software package created to simulate the fuel pin sag test will be presented and compared to the experimental results.

EXPERIMENTAL

Material, Equipment and Instrumentation

The fuel pin used was an outer pin taken from a 37-pin bundle with staggered bearing pads. The fuel sheath was internally coated with CANLUB® and filled with standard natural uranium dioxide pellets with double dishes. It was autoclaved at 10 MPa and 300°C for 10 hours to ensure uniform pellet-to-sheath gap for comparison with other fuel pins.

Axial and circumferential temperature gradients may significantly influence the fuel pin deformation behavior. The temperature distribution was monitored using nine type-K thermocouples attached by spot welding the individual wires directly to the fuel pin sheath. The thermocouple attachment locations are shown in Figure 1.

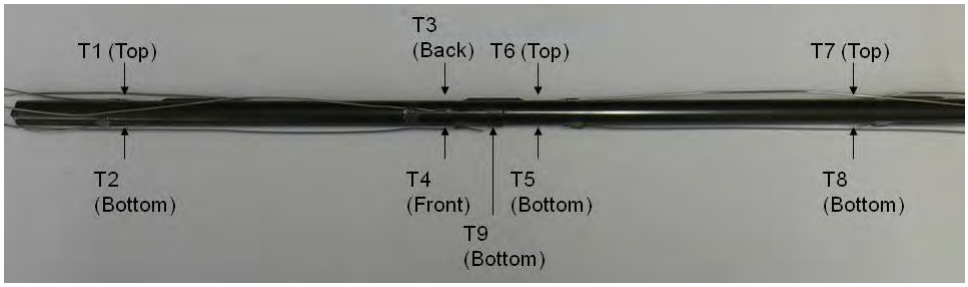

Figure 1. Thermocouple locations for the fuel pin sag test.

The fuel pin was heated using a 5 kW infrared parabolic furnace from Research, Inc. of Eden Prairie, MN, USA. The power supplied to the furnace lamps was controlled using one of the thermocouples attached to the fuel pin sheath. The furnace was equipped with a fused quartz tube with stainless steel end-caps secured to a rigid external mounting base. Argon saturated with water vapor was pumped through the fused quartz tube to help maintain an oxide coating during the test, which minimized inaccuracies associated with specular reflection from the sheath surface.

The fuel pin was placed in the furnace tube on a tubular fused quartz support with a wide slot cut in the bottom to minimize optical interference. The fuel pin was supported near each end on the top edge of a V-shaped cutout with a width of about 1 mm. The separation between the support locations was 474 mm, about 8 mm from each end of the fuel pin. The fuel pin was simply supported (no axial or rotational constraint other than 1 mm sheathed thermocouples).

Surface position coordinates of the bottom of the fuel pin were measured using a Micro-Epsilon scan CONTROL2700-100-B laser light-stripe sensor, which was modified by the substitution of a blue laser for the red laser normally used in this sensor. The customized version of the sensor was constructed by Micro-Epsilon (Germany) to be able to measure targets with surface temperatures up to 1200°C. The light-stripe sensor was moved along the sample at 200 mm/s using a positioning table with a rotary encoder, with 15 mm acceleration and deceleration zones at each end of travel, and a 0.1 s pause between sweeps to minimize vibration.

The light stripe laser was targeted onto the bottom of the specimen through a slot between the furnace clamshells. The profile of the fuel pin was measured at a rate of 25 profiles per second (irrespective of the sensor position), implying that the profiles were measured at intervals of about 8 mm axially along the fuel pin. The sensor axial location was known within 0.1 mm. The horizontal resolution of the light-stripe sensor in this test was approximately 0.15 mm. The profile data captured all vertical or horizontal displacements of the furnace tube or supports, or difference between the fuel pin major axis and the motion axis of the sensor, because it measured two-dimensional profiles along most of the length of the fuel pin. Positional and temperature data were captured by a data acquisition program built using

the National Instruments LabView 2010 DAQmx package and the software developer's kit written for the light-stripe sensor by Micro-Epsilon (Germany).

Figure 2 depicts the experimental set-up and instrumentation used for the high temperature fuel sag test presented in this paper.

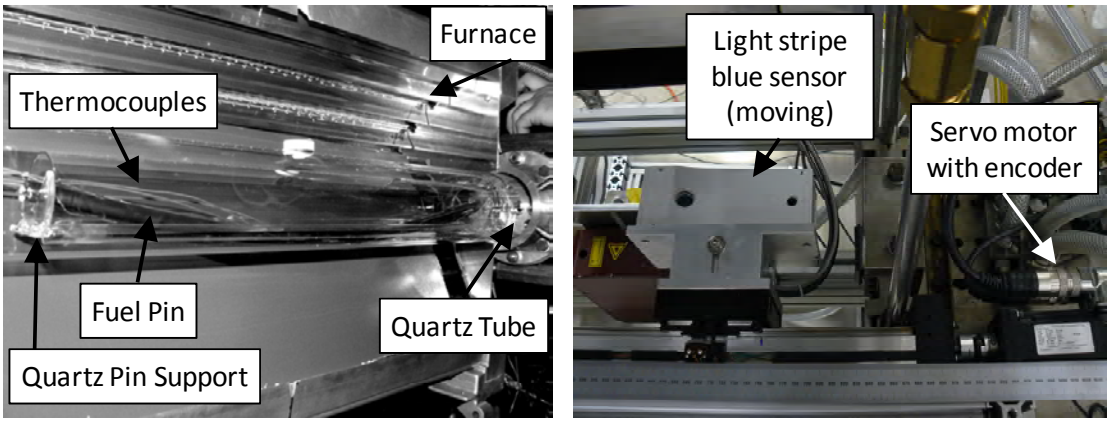

Figure 2. Experimental set-up for a high temperature fuel sag test using an infra-red parabolic furnace.

Experimental Conditions

The planned temperature program is outlined in Figure 3. The fuel pin was heated to 300°C at 1°C/s and held there for 120 s, followed by two repetitions of heating to 800°C at 1°C/s, holding for 120 s, and cooling to 300°C. In a third heating cycle the fuel pin was heated to 800°C, held at 800°C for 120 s, then heated to 1000°C at 1°C/s and held for 60 s, followed by cooling to room temperature.

Measurements from the furnace control thermocouple (T4) located near the pin mid-plane are also reported in Figure 3. The temperature readings of all thermocouples were generally within 25°C, with maximum differences of 58°C during the 1000°C plateau and 103°C during the cooling from the 1000°C plateau. Therefore it was concluded that the fuel pin temperature was fairly uniform spatially, as intended.

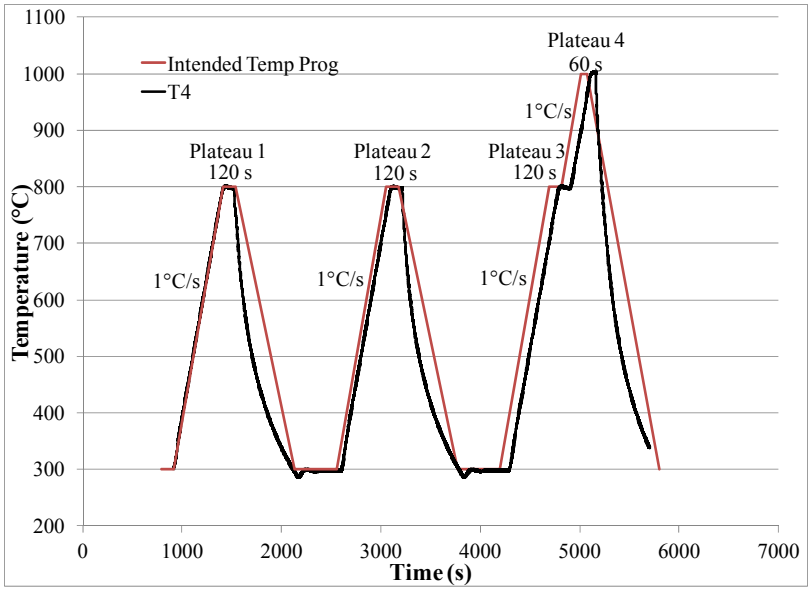

Figure 3. Planned temperature program and measured sheath temperature near the fuel-pin mid-plane.

EXPERIMENTAL DATA ANALYSIS

Discrete measurements of positions of points on the fuel pin surface were made with reference to a 3D Cartesian coordinate system. Positions of points in space were represented by sets of 3 distances from a fixed origin: x along the dimensioning system line of travel, y across the fuel pin, and z in the vertical direction. The position measurements were correlated with discrete measurements of time, t. The light-stripe sensor data for this test had the form of lateral profiles $\{t_p, x_p, \{y_i, z_i\}_p\}$, where the profile ordinal p ran from 1 to 138,963, and the point ordinal i ran from 1 to $n(p)$. The number of points in individual profiles varied over the interval $1 \leq n(p) \leq 114$.

During this high temperature sag test, 8,993,417 spatiotemporal coordinate values represented by $\{t_p, x_p, \{y_i, z_i\}_p\}$ were collected. Techniques applied to analysis of the collected data are outlined below.

Description of Experimental Data Analysis

The goal of the analysis was to parameterize the data in a manner that would provide useful quantitative information on time- and axial-position-dependent behavior of profile positions and shapes, during deformation. The intended purposes were to improve understanding of the phenomenon of fuel-pin deformation and to provide values of quantities suitable for comparison with ANSYS-based models.

Commensurate with the large amount of data to be analyzed, a relatively simple parameterization was selected. Individual profiles represented by the data were assumed to have elliptical geometry, with the center of the ellipse, $\{y_0, z_0\}$, providing horizontal and vertical parameters of position in the $\{y, z\}$ plane and the semimajor and semiminor axes, a and b respectively, providing shape parameters. The axes of the ellipse were assumed to be parallel to the coordinate axes, with a parallel to the z axis and b parallel to the y axis (Figure 4). The parameters were evaluated numerically by first filtering noise and artifacts from the data and then fitting ellipses to the filtered data for each profile p. From the time- and axial-position-dependent position parameters, lateral and vertical components of deflection were computed. For the purposes of comparison with ANSYS-based models, the vertical component of deflection was an essential output from the experimental analysis.

A specialized data filtering algorithm was used to detect whether or not a data point corresponded to a position on a fuel pin surface. Noise and extraneous data such as the position measurements associated with the thermocouple leads, wires, spacer and bearing pads were rejected from the useful data set. An example of the results of applying the filtering algorithm is shown in Figure 5.

For each profile, an ellipse was fitted to the points judged to be on the fuel pin surface. The projection of the light-stripe onto the cylindrical fuel sheath surface would give an arc of a circle if the stripe was perpendicular to the fuel sheath (a good approximation at the beginning of the test). Later in the test, when the pin had sagged, elliptical profiles were expected in regions where the stripe was no longer perpendicular to the cylindrical axis of the fuel pin.

The parameters of an ellipse were fitted to a set of points in a profile by minimizing the arithmetic mean of the distance Δr from the points to the curve of the ellipse (Figure 4). The coordinates of a point $\{y_e, z_e\}$, lying on the curve of an ellipse in the $\{y, z\}$ Euclidean plane, satisfy Equation 1 below, where the ellipse is centered at $\{y_0, z_0\}$, the semimajor axis of the ellipse a is aligned with the z coordinate axis, and the semiminor axis b is aligned with the y coordinate axis.

$$\frac{(z_e - z_0)^2}{a^2} + \frac{(y_e - y_0)^2}{b^2} = 1 \qquad (1)$$

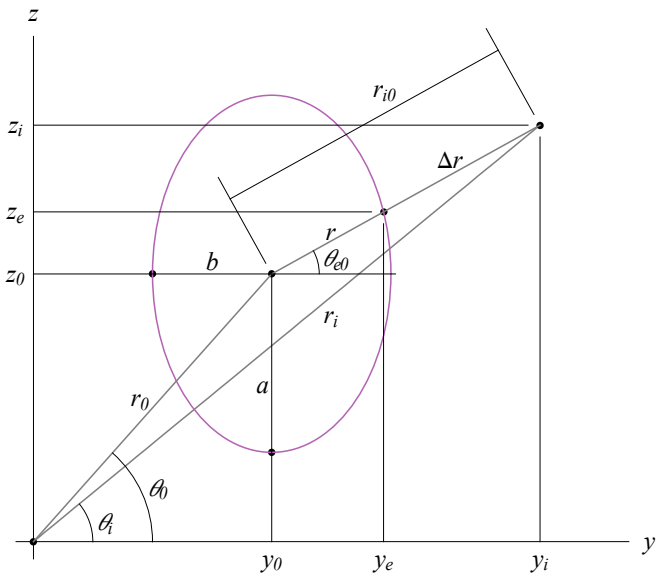

Figure 4. Geometric sketch with symbols used for fitting ellipses to set of data points judged to be on the fuel-pin surface.

A data point, with measured Cartesian coordinates $\{y_i, z_i\} \neq \{y_0, z_0\}$, or polar coordinates $\{\theta_{e0}, r_{i0}\} \neq \{\theta_{e0}, 0\}$ with respect to the center $\{y_0, z_0\}$ of an ellipse, is a radial distance Δr from the curve of the ellipse, where Δr is given by Equation 2 below:

$$\Delta r = r_{i0} - r \tag{2}$$

The shortest distance between an arbitrary point and the curve of an ellipse is the lesser of the two distances measured along a line coincident with the point and orthogonal to a tangent of the curve. Assuming that the eccentricity of an ellipse to be fitted is small, the curve of an ellipse approximates that of a circle for any value of θ_{e0}, and therefore the radial distance Δr approximates the shortest distance between the point and the curve of the ellipse. Accordingly, for a profile comprised of n data points, an ellipse may be fitted to the data by minimizing the arithmetic mean $\overline{\Delta r}$ of the absolute values of the n radial distances with respect to the ellipse parameters $\{a, b, y_0, z_0\}$ (Equation 3):

$$\overline{\Delta r} = \frac{1}{n}\sum|\Delta r| = \frac{1}{n}\sum_{i=1}^{n}|r_{i0} - r| \tag{3}$$

Using Equation 1, the law of cosines, and trigonometric relations, expressions for r_{i0} and r in terms of the ellipse parameters and data-point Cartesian coordinates are obtained (Equations 4 and 5):

$$r_{i0} = \sqrt{{y_0}^2 + {z_0}^2 + {y_i}^2 + {z_i}^2 - 2\sqrt{{y_0}^2 + {z_0}^2}\sqrt{{y_i}^2 + {z_i}^2}\,\cos\left(\tan^{-1}\frac{z_0}{y_0} - \tan^{-1}\frac{z_i}{y_i}\right)} \tag{4}$$

$$r = \left(\frac{\left(\frac{y_0 - y_i}{b}\right)^2 + \left(\frac{z_0 - z_i}{a}\right)^2}{(y_0 - y_i)^2 + (z_0 - z_i)^2}\right)^{-1/2} \tag{5}$$

An example of an ellipse fitted to a data profile, by minimizing $\overline{\Delta r}$ (Equation 3) with respect to the ellipse parameters appearing in Equations 4 and 5, is shown in Figure 5.

Elapsed Time	t (s)	420.168
Axial position coordinate	x (mm)	249.91
Ellipse center coordinates	y_0 (mm)	−20.39
	z_0 (mm)	373.45
Semiminor axis	b (mm)	6.56
Semimajor axis	a (mm)	6.55

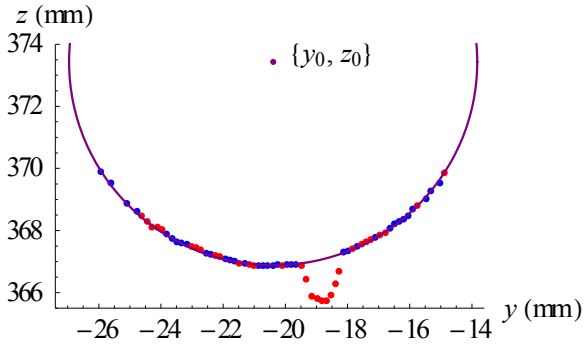

Figure 5. Ellipse (purple) and ellipse parameters fitted to filtered data (blue) in a profile.

The $\{t_p, x_p\}$ spatiotemporal grid upon which the data was collected was unstructured, and therefore multivariate first-order approximate interpolation functions were derived for position parameters and shape parameters, in order to permit their differentiation and integration. In particular, the interpolation functions were used to generate time- and axial-position-dependent values of the lateral and vertical components of deflection $\{\Delta y_0, \Delta z_0\}$, by subtracting initial "reference" values of position parameters $\{y_0, z_0\}_{ref}$ from subsequent interpolated values. Changes in the shape parameters a and b were generated similarly. From pairs of discrete values of time and T4 thermocouple-temperature ϑ, a third-order interpolation function was derived.

The interpolation functions for temperature, and position and shape parameters, were used to plot and visualize the results of the experimental data analysis, and to generate discrete datasets comprised of correlated values of $\{t, x, \Delta y_0, \Delta z_0, \Delta a, \Delta b, \vartheta\}$ on structured $\{t, x\}$ grids, appropriate for comparison of the experimental results with ANSYS-based model results.

Results of Experimental Data Analysis

The discussion of results concerns only vertical deflections measured during successive temperature transients, because horizontal deflections and changes in fuel pin cross-section were relatively small. The principal results of the experimental data analysis are summarized graphically in Figures 6 and 7, which plot the temperature and the vertical component of the change in the position parameter Δz_0, as approximate interpolating functions of time t and axial-position-coordinate x.

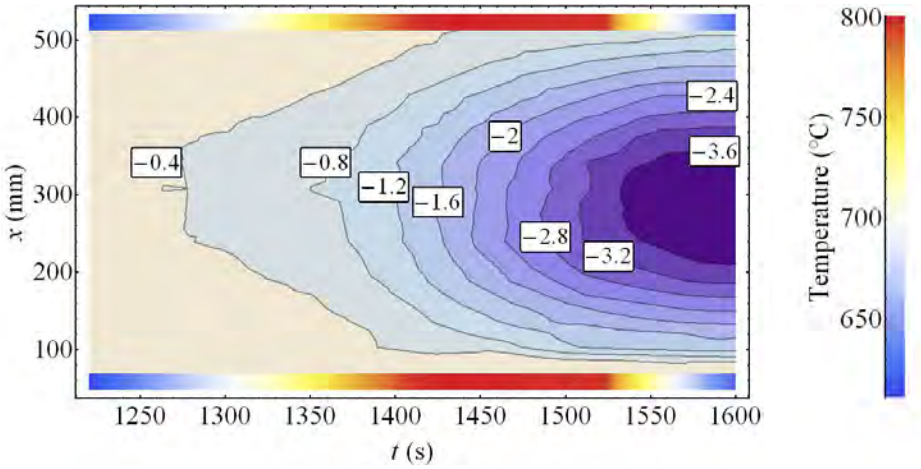

Figure 6. Labeled contour plot of vertical deflection Δz_0 (mm) showing dependence on time, temperature, and axial position, from experimental analysis, during the first temperature cycle to 800°C.

Temperature is indicated by respective color maps, shown by the scales on the right sides of Figures 6 and 7. Figure 6 shows as a contour plot how the full unsupported length of the fuel pin (474 mm) deflected during the time interval of the first temperature cycle to 800°C. Figure 7 depicts, as a 3D plot, how the full unsupported length of the fuel pin (474 mm) deflected during the entire time of the temperature program shown in Figure 3. The scale along the Δz_0 axis is exaggerated with respect to that along the x axis, in order to more clearly show the behavior of the deflection.

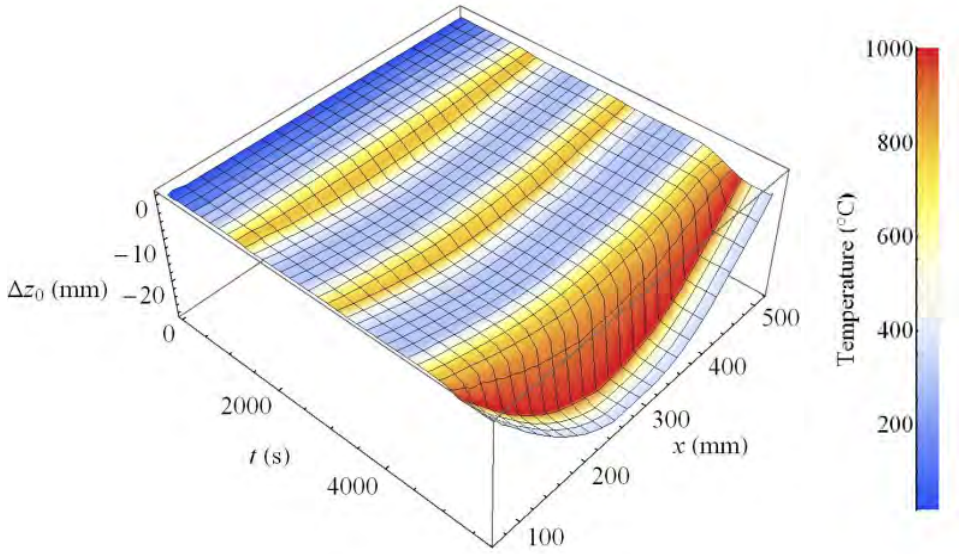

Figure 7. Vertical deflection, from experimental analysis, showing dependence on time, temperature, and axial position.

Table 1 shows values of physical quantities obtained near the axial midpoint of the unsupported fuel-pin span (see also Figure 9). During each temperature cycle to 800°C, the deformation became detectable at about 760°C, which is approaching the temperature range of Zircaloy-4 phase transition from α to β phase (~820°C to 980°C). The sag rate for the first cycle to 800°C was greater than the rates for the second and third cycle. The sag rate increased significantly at temperatures above 874°C. The maximum Δz_0 vertical displacement values were estimated using a linear regression function calculated over a few hundred seconds during each temperature plateau.

Table 1: Initial sag temperatures and sag rates from analysis of data measured by a light-stripe laser sensor and T4 thermocouple located near the mid-plane of fuel pin.

	Plateau 1 800°C	Plateau 2 800°C	Plateau 3 800°C	Plateau 4 1000°C
Initial sag temperature before plateau [°C]	763±10	756±10	761±10	874±10
Sag rate at 800°C [mm/s]	0.019±0.002	0.012±0.002	0.010±0.002	0.20±0.01
Max vertical deflection Δz_0 [mm]	3.95±0.02	6.41±0.02	N/A	≥ 28.42*

*The deflected fuel-pin reached contact with quartz furnace tube at $\Delta z_0 = 28.42$ mm.

MODELING

Modeling vertical or horizontal deformations of a CANDU® fuel pin poses a significant challenge as the behavior is determined by the interaction of the fuel pellets with the sheath and each other. If the fit between the fuel pellets and the sheath is very tight, then the pin may be simulated as a simple solid beam; conversely, if the pellets are loose within the sheath then the pin may be modeled as a weighted hollow tube. Most situations lie between these two conditions and the sliding of the fuel pellets within the sheath and the contact between individual pellets must be included in the model. The situation is further complicated if the imposed loads or the temperature of the fuel pin is such that plasticity of creep behavior of the Zircaloy sheathing must be considered. These phenomena are dependent on the stress state of the sheath and the presence of the fuel pellets causes sheath-stress heterogeneity, particularly at the pellet-to-pellet interfaces. Further, the differences in coefficient of thermal expansion of the fuel and sheath materials mean that the interface pressures between the pellets and sheath, and hence the interaction between these components, is temperature dependent.

Model Description

A solid 3D finite element model of a fuel pin was created using the commercially available ANSYS finite element package. 3D models of each pellet and the sheath were created as separate components and then contact elements were used to simulate their interactions. The fuel pin was modeled with two planes of symmetry, one axial and one transverse, reducing the model size to one quarter that of a full fuel pin.

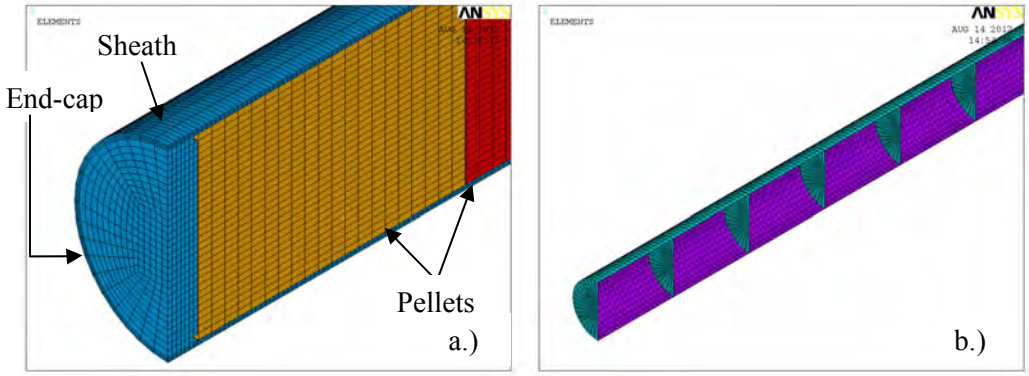

Figure 8. ANSYS model geometry: a.) Finite element mesh used; b.) Pellet-to-pellet and pellet-to-sheath contact elements.

Hexahedral elements of ANSYS type SOLID 226 were chosen for their stability in non-linear mechanical simulations. For these simulations, a uniform time-dependent temperature was imposed as a boundary condition on the model, although the model does have the capability to be used in fully coupled thermo-mechanical calculations. Details of the finite element mesh used are shown in Figure 8 a.). The mesh used for the end-cap is identical to the one for the fuel pellet.

Contact between the fuel pellets and the sheath, as shown in Figure 8 b.), was modeled using standard ANSYS contact and target elements of the ANSYS type CONTA174 and TARGE170. The augmented Lagrange solution method was used which is a modified form of the widely used penalty method (see the ANSYS 13.0 online users' manual).

The temperature dependent material properties of both the UO_2 fuel and Zircaloy sheathing were derived from the models used in the CANDU® Industry Standard Tool fuel analysis code ELOCA, Williams (2005). It was necessary to simplify the high temperature Zircaloy creep model used in the

ELOCA code so that it could be readily implemented in the ANSYS model. Only the diffusional component of the ELOCA creep model was used as shown in Equation 6:

$$\dot{\varepsilon} = F\left(\frac{\sigma_a}{d}\right)^m e^{\frac{-Q}{T}} \tag{6}$$

where $\dot{\varepsilon}$ is the creep rate (s^{-1}), σ_a the applied stress (MPa), d the grain size (μm), T the temperature (K), Q the activation energy (K), F is a temperature and material dependent factor, and m is an empirical constant. This component of the creep model has the same form as the standard Norton expression for secondary creep which is a standard ANSYS model option, and could be readily implemented by simply supplying the correct coefficients to the ANSYS model.

Although the model has the potential for fully coupled thermo-mechanical simulations, the slow transient times and external heating method used in these experiments meant that the temperature within the fuel pin could be assumed to homogeneous and supplied as a time dependent boundary condition to a purely mechanical simulation. The temperature transients shown in Figure 3 were simulated. Suitable mechanical constraints were applied to the planes of symmetry and the pin was assumed to be simply supported at the appropriate locations on the bottom surface of the sheath.

Model Results

Two simulations were conducted and are shown in Figure 9.

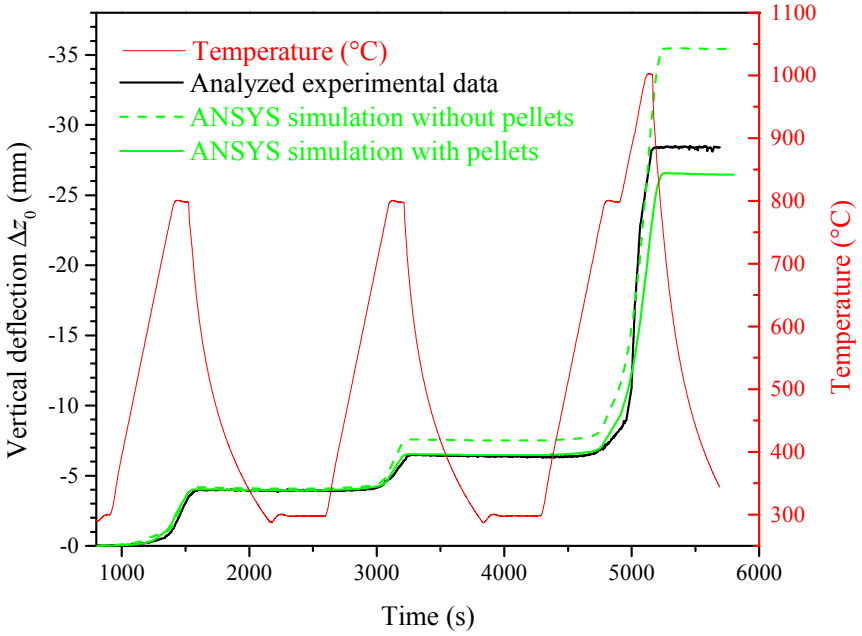

Figure 9. Experimentally measured vertical deflection near mid-plane of the unsupported fuel-pin span ($x = 282$ mm) compared with ANSYS-based simulations.

In the first simulation the fuel pin was simulated as a hollow sheath with the density adjusted to simulate the weight of the fuel pellets. This is equivalent to assuming that the presence of the pellets does not influence the stiffness of the pin. As seen in Figure 9 this model performed well for the first temperature transient, but predicted too much deflection for the second temperature transient.

The second simulation included the pellets as full 3D entities which interacted with the sheath and each other via contact elements. In this case the simulation performed well for the first two

transients. It is interesting to note that although the first two temperature transients were of similar temperature and duration, the change in deflection during the second transient was smaller than the first. This behavior was only captured when the full interaction of the pellets and sheath was simulated. The high temperature of the third transient resulted in a high creep rate and the uncertainties in the creep model are the likely explanation for the differences between the results of the experiment and the simulation.

CONCLUSION

An experiment was conducted in which a CANDU fuel pin instrumented with nine type K thermocouples was subjected to multiple heating/cooling cycles to 800°C and to 1000°C with a heating rate of 1°C/s.

The experiment successfully demonstrated the capability of measuring online high-resolution spatiotemporal behavior of a fuel pin subjected to high temperatures using a non-intrusive dimensioning system. Analysis of the results provided valuable and reliable data for the development of models to simulate fuel pin deformation behavior. Models incorporating the full interaction of the pellets and sheath provided the best results in ANSYS-based simulations of the experiment.

The methods developed in relation to the single fuel pin, presented in this paper, are currently being applied to test an entire CANDU® 37-pin bundle in a dedicated, unique facility.

ACKNOWLEDGEMENTS

The authors acknowledge CANDU® Owners Group for funding of the experimental work and Atomic Energy of Canada Limited for funding the data analysis and modeling. The technical expertise of M.D. Gauthier, R.T. Peplinskie, J. Sheedy, P.A. Moss, A. Clouthier, M.L. Cusick, C. Fraser, A. West, A. Belov and B. Smith, is gratefully acknowledged. B.W. Leitch and T. Nitheanandan provided valuable guidance with regard to the overall test program.

REFERENCES

Hughes, T. J. R. and Allik, H. (1969). “Finite Elements for Compressible and Incompressible Continua,” *Proc., Symposium on Application of Finite Element Methods in Civil Engineering*, ASCE, Nashville, TN, 27-62.

Kohn, E., Hadaller, G.I., Sawala, R.M., Archinoff, G.H., and Wadsworth, S.L. (1985). “CANDU Fuel Deformation during Degraded Cooling: Experimental Results,” *Proc., 6th International Conference on CANDU Fuel*, Ottawa, ON, 16.39-16.45.

Walters, L.C. and Williams, A.F. (2003). “Fuel Bundle Deformation Model,” *Proc., 8th International Conference on CANDU Fuel*, Honey Harbour, ON, 452-463.

Williams, A.F. (2005). “The ELOCA fuel modeling code: past, present and future,” *Proc., 9th International CNS Conference on CANDU Fuel*, Belleville, ON, 1-14.